

Evolution of Swarna estuary and its impact on braided islands and estuarine banks, Southwest coast of India

Kumar Avinash^{1,2} K.S. Jayappa^{1*} P. Vethamony³

¹*Department of Marine Geology, Mangalore University, Mangalore – 574 199, India*

²*EEZ Group, National Centre for Antarctic & Ocean Research, Goa – 403 804, India*

³*Physical Oceanography Division, National Institute of Oceanography, Goa – 403 004, India*

Tel: +91-824-2284343

Fax: +91-824-2287289

E-mail: ksjayappa@yahoo.com

Abstract

Qualitative and quantitative evolution of the Swarna estuary, during the past 38 years (1967–2005), has been analysed by integrating the results of field surveys, satellite images, hydrodynamic modelling and topographic data in GIS context. Significant changes in erosion/accretion patterns of the estuarine banks, inlet configuration and adjacent spits, and origin, morphology, orientation and areal extent of fifteen braided islands have been estimated. Hydrodynamics of the region is studied through modelling, and probable flow pattern that is responsible for morphological changes is discussed. The simulated flow patterns indicate that current speeds are of the order of 10–20 cm/s inside the estuary and of the order of 40 cm/s at the mouth. The Right bank (Rb) of the estuary is subject to net erosion and the Left bank (Lb) is subject to net accretion. On an average, 20–30% of the area of all braided islands would be flooded, if the water level rises by 0.7 to 1.0 m. Islands of this estuary are morphologically very dynamic (migrating towards north, northeast and southwest directions) and subject to net accretion, whereas only one island (i.e., the Padu) has lost its major portion of landmass. A conceptual Inverse Distance Weighted (IDW) interpolation model has been generated and evaluated possible flooding on the estuarine shoals and braided islands, due to heavy rainfall and/or sea-level rise. The model reveals that the possibility of flooding will be higher for those islands which are located close to the Rb than those close to the Lb.

Keywords: *Coastal and Estuarine Processes, Braided Islands, Hydrodynamic Modelling, Impact of Floods, Remote Sensing and GIS.*

Introduction

Coastal geomorphological changes are influenced by geological, meteorological and oceanographic factors. The processes involved in the evolution of coastal geomorphological system are necessary to know the sources of sediment supply to the littoral region, the sinks and sediment transport in the littoral zones (Chandramohan et al. 2001). Signature of sea-level changes is imprinted in coastal/tidal zones and estuaries (Knebel et al. 1988; Allen and Posamentier 1993; Dalrymple and Zaitlin 1994; Achyuthan and Baker 2002). Estuarine environment is characterized by temporal changes that occur due to hourly (tide) to seasonal variations (river discharge). Any modification to hydrological regime (tide, wave, current and river discharge) or sediment supply affects the estuarine evolution and alters the previously-achieved equilibrium system (Jouanneau and Latouche 1981). To monitor such changes synoptic analyses are imperative (Menon et al. 2006). When hydraulic forces of inland rivers and hydrodynamic regime of coastal ocean are of equal intensity, the waves and currents quickly rework the river-borne sediments. The resultant coastline will have marine built landforms with spits and barriers growing in the direction of dominant littoral drift (Write and Coleman 1973; Chakrabarty 1991; Sastri et al. 1991). Studies on the evolution of these coastal landforms not only help in understanding the morphogenetic set-up of the terrain, but also aid in preparation of management programmes pertaining to protection of coastal region (Chen and Rau 1998). The combination of remote sensing and GIS forms a powerful framework for multi-scale spatial data acquisition and synthesis that are essential for characterizing the space–time continuum of a complex estuarine ecosystem (Yang 2005).

Fluvial/estuarine islands are common feature of active river system and estuarine processes that store the information concerning the geomorphic histories that characterised their drainage basin. There are 15 (10 small, 3 medium and 2 large) braided islands (locally called as *Kudrus*) in the Swarna estuary (Fig. 1). These islands are the product of avulsion (the sudden separation of land by a flood or by an abrupt change in the course of a stream), rapid and gradual channel incision, channel migration, dissection of both rapidly and slowly deposited bed sediment, and a vegetated surface or behind a channel obstruction. Some of them change dynamically and morphologically due to coastal and estuarine processes and anthropogenic activities. Topography of low-lying coastal areas is a primary determinant of their susceptibility to inundation. Therefore, a high-resolution topographic mapping is necessary (Titus and Richman 2000). Lack of high-resolution maps makes it difficult to quantitatively assess the people and property at risk from flooding and sea-level rise. Heavy rainfall

and rising water-level in the estuary during the southwest monsoon season (June-September) lead to flooding and erosion of these islands.

The present study deals with morphological changes of spits adjacent to estuarine mouth, erosion/accretion patterns of estuarine banks and islands in the estuary during the past 38 years (1967-2005). An attempt has been made to estimate the evolution of braided islands, and probable areas which could be flooded during heavy rainfall, high tides and/or sea-level rise.

Area of Study

The study area extends from 13°23'30" N to 13°28'30" N latitude and 74°41'55" E to 74°45'00" E longitude of the Swarna estuary (Fig. 1). The river Swarna originates at an elevation of about 460 m in the *Sahyadri* (Western Ghats) hill ranges and flows westward to a distance of ~80 km. The upstream end of the Swarna river receives freshwater influx during the southwest monsoon season and very little during rest of the year. The Swarna and Sita rivers are the main sources of sediment supply to the coastal sea.

Physiographically, the estuary falls in the coastal plain and the weather is hot (average 30°C) and humid most part of the year. Climatologically, the study area experiences three seasons – southwest monsoon (June-September), northeast monsoon (October-January), and inter-monsoon (February-May). The average annual rainfall is ~3,930 mm. Of this, about 82% of the rainfall is received during the southwest monsoon and the rest during northeast and inter-monsoon months (Jayappa et al. 2003). Hence, the estuary is freshwater dominated during June-September and seawater dominated in the rest of the year. Winds are strong (10-18 km/h) and mainly in the westerly or southwesterly direction during the southwest monsoon, and in the rest of the year, northeasterlies (in the mornings) and westerlies / northwesterlies (in the afternoons).

Waves and tides

Waves along this coast are generally low during pre-monsoon and post-monsoon seasons. During pre-monsoon season, the significant wave height ranges up to 1.2 m, whereas it goes upto 1.5 m during post-monsoon season. The mean wave period ranges between 3 and 6 s during the above seasons. However, significant wave heights range upto 4.0 m (observed off the coast of Mangalore) during SW monsoon in the west direction. Mean wave period ranges between 5 and 10 s during this season. The mean wave direction during pre-monsoon season is between W and NW. Local wind

seas are dominated in this region during pre-monsoon season. Waves during post-monsoon season are mainly from SW direction, which are dominated by distant swells.

Udupi-Mangalore region experiences mixed semidiurnal micro-tides. Unlike the northwest coast of India, the southwest coast shows not much variation in water levels during spring and neap periods. The mean sea-level off Mangalore is of about 1m; the mean low water spring is between 0.5 and 1.0m; high water level in spring time is in the range from 1.5m to 2.0m. During neap period, the low and high water levels range from 0.5m to 1.0m and from 1.0 to 1.5m, respectively (Sanil Kumar et al. 2006).

Materials and Methods

The methodology is directed to evaluate spit morphological changes on either side of the estuarine mouth, islands and banks of Swarna estuary. Relevant spatial and non-spatial field data were collected during 2006-2008. Time series satellite data were processed and mapped using ERDAS IMAGINE v. 9.1 and ArcGIS 9.0 software, respectively. Data processing methodology is described below. The littoral drift pattern and its impact on the morphology of spits and estuary have been extracted from satellite images. In order to understand the physical processes acting in the study area, hydrodynamic modelling was carried out using MIKE-21 HD modelling system.

Data products and image rectification

Cloud free digital images of Indian Remote Sensing Satellite (IRS)-1C/1D/P6 of Panchromatic (PAN, 5.8 m resolution) and Linear Imaging Self Scanner (LISS-III, 23.5 m resolution) were acquired (during low-tide) for January 1997 and December 2005, and analysed using digital image processing techniques. To minimise the inaccuracy in image rectification and enhancement, both PAN and LISS-III images have been subsetted based on our area of interest. The Survey of India topographic map (48 K/11) of 1967 edition (1: 50,000 scale) was used as ancillary data. All the satellite images were geo-referenced by taking more than 30 ground control points (GCPs, at connecting bridges, road junctions, rock outcrops etc.) selected uniformly across the study area, from topographic map as well as GPS recorded ground points, on the IRS images using ERDAS IMAGINE v 9.1 software and a polynomial transformation of the first (affine) order was derived. Overall accuracy of the transformation, expressed as root mean square errors (RMSEs) for geo-referenced images was not permitted to exceed more than 0.2 pixel (or <0.1 pixel for Map-to-PAN registration, where GCPs can be more accurately located) corresponding to approximately <2.5

m (Map-to-LISS) to <0.6 m (Map-to-PAN) on the ground. After geo-referencing in geographic (lat/long) projection, a nearest neighbour interpolation method (as no change occurs in pixel values) was used to rectify and resample the images into a Universal Transverse of Mercator (UTM) projection, WGS 84, Zone 43 North.

In order to precisely delineate and estimate the areal extents of coastal landforms, - spits, estuarine banks and braided islands - high resolution (5.8 m) false colour composite (FCC) images have been generated by merging/stacking the layer of PAN and LISS-III image of January 1997. Similar procedure is also followed for PAN and LISS-III images of December 2005. In the present study, spatial error among the multi-dated satellite images due to tidal variation, weather conditions and pixel variations during data acquisition have been generalized, using the methods carried out earlier by Avinash Kumar et al. (2010).

Analysis of estuarine morphology

In order to delineate the land/estuary/sea boundary, and compute the changes in position of estuarine banks/mouth and islands, the image IRS 1C/1D, PAN and IRS 1C/P6, LISS-III of infrared spectral band-4 (1.5-1.7 μm) were employed. Several methods are in use for deriving coastline/estuarine position from remote sensing data such as post-classification comparison, change vector analysis and image differencing (Weismiller et al. 1977; Quarmby and Cushnie 1989; Singh 1989; Lambin and Strahler 1994; Lillesand and Kiefer 2000) were followed. Due to difference in the reflectance of the visible channels in water versus land, the differencing technique was applied to the multidated IRS images to highlight the littoral drift pattern and morphological changes. Vector layers of estuarine mouth, adjacent spits and islands were created using topographic maps and satellite images. These layers were superimposed in order to estimate spatial and temporal morphological changes using ArcGIS v 9.0 software. To estimate the width and areal extent of erosion/accretion pattern, the Right bank (Rb) and the Left bank (Lb) have been divided into 20 and 15 blocks, respectively. The width of each block was measured at every 70 m interval and their variations were studied. Present orientation, shape, extent (length and width) and ground elevation from mean sea-level (MSL) are investigated and recorded for all the braided islands of the Swarna estuary, during our field surveys conducted in November 2008.

Current patterns and hydrodynamic modelling

Current measurements conducted during different seasons for two years have been analysed to understand the prevailing flow pattern off Udupi region. Current Meters (RCM-7) were moored on

12 May 1997 off Swarna estuary at 13°28'N and 74°38'E with a clearance of 2 m both from surface and bottom (water depth of 12m) and retrieved on 27 May 1997. The current meters were set to sample the data at every 10 minutes interval. To understand the flow pattern during winter season, the current measurements were again continued at the same location during 9-28 January 1998. Currents were resolved into U-Component (east-west) and V-Component (north-south) in order to quantify the alongshore and onshore-offshore dominance of currents which influence the sediment transport (Fig. 2).

MIKE-21 HD (hydrodynamics) model has been used to simulate water levels and currents off Swarna region during 19-20th April, 2007. HD solves two dimensional shallow water equations of momentum and continuity as the maximum depth of the area considered is < 50 m and the currents are influenced by tides. Cartesian coordinate system is used in the model with high resolution grid spacing of 250 m to accommodate the coastal features. The boundary of the model is considered as Malpe in the south and Kundapur in the north (Fig. 3). The depth contours are digitized from the Naval Hydrographic charts. The maximum depth included in the model domain is 50 m. The model was forced by applying water level variations along the open boundaries and winds on the sea surface.

Surface interpolation model for flood prediction

Surface interpolation is an effective method of bringing points and areal data in a common spatial framework, if the measured property is inherently a continuous variation in space. Comprehensive reviews of existing surface interpolation methods can be found in Laurini and Thompson (1992), Bonham-Carter (1994) and Burrough and McDonnell (1998). In all, more than 580 elevation points were measured at 50 m interval using Leica 200 GPS all along the periphery and across the braided islands during the field surveys. These elevation points were post-processed and differentially corrected as per Cook and Pinder (1996), and then elevation maps were created using Inverse Distance Weighted (IDW) interpolation tool in 3D Analyst module of ArcGIS software. The IDW is a well-known interpolation method, where weighting is assigned to data using the inverse separation distance to a power as a weighting function (Aguilar et al. 2007). A weighting power parameter of 2 was used in this case, and validated with a RMSE <0.1 m. This tool creates a continuous surface from discrete samples like elevation values. The interpolated values of IDW surfaces were the weighted average of a set of nearby points; the influence of nearby points is greater than that of distant points (inverse of the distance).

Results and Discussion

Coastal and estuarine processes on estuarine morphology

Natural processes and anthropogenic activities, such as construction of major/minor ports, vented dams across the river channel, industries; sand mining from river and estuarine bed; aquaculture farming, and other human intervention in the form of coastal defenses, play a major role in setting estuarine morphology. In order to understand hydrodynamics of the region, available current meter data of the nearby location at a water depth of ≈ 12 m was subject to flow pattern analysis. Figure 2 indicates that flow during inter-monsoon season is predominantly between south and southeast with maximum current speeds of the order of 35 to 40 cm/s. There were frequent spells of current reversals with weak northerly currents. Currents have been resolved into u components (east-west) and v components (north-south) to get the dominant flow responsible for estuarine morphology. Though currents are in general parallel to the coast and parallel to the depth contours, a small onshore current component (u-east) is present, which can transport sediment materials towards the estuary.

Further, we have conducted simulations for hydrodynamics using MIKE-21 HD model. Predicted tides at Malpe and Kundapur were given as boundary conditions, and wind data collected using autonomous weather station was used as input data. Typical flow patterns for flood and ebb phases of the tide are shown in Fig. 3. The simulated flow is typical of any dynamic tropical estuary dominated by tidal currents. Current speed remained at an average speed of about 10-20 cm/s inside the estuary; however strong currents of about 40 cm/s prevailed at the mouth. Flooding and drying occurred in semidiurnal period with vast areas of estuarine channels getting exposed during ebb phase. Tidal pools were formed in the estuary during the ebb phase as water drained out from areas of zero elevation, and estuarine channels disrupting the connectivity of the estuary with the coastal waters. Probably, this may be one of the reasons for some of the islands/spits/shoals getting exposed.

Hydrodynamics associated with sediment transport modifies estuarine morphology. The analysis shows that drastic morphological changes have taken place in the estuarine mouth between 1967 and 2005 (Figs. 4 and 5). Comparison of position and width of the estuarine mouth during the past 38 years reveals that width of the mouth remained almost the same, but its position shifted towards southeast by ~ 560 m. The reasons are as follows: (i) accretion and growth of the Kodi Bengre spit by ~ 560 m towards southeast and (ii) complete erosion of distal end of the Oddu Bengre spit by ~ 470 m during this period (Fig. 4). The estimated net accretion is about 82 acres and erosion

is about 30 acres at the distal ends of Kodi Bengre and Oddu Bengre spits, respectively (Figs. 4 and 5). The dynamic changes occurring in the estuarine mouth are primarily due to currents and southerly littoral drift (Jayappa et al. 2003). Therefore, the accretion on the northern side of the inlet (i.e. along Kodi Bengre spit) and erosion on its southern side support the observation of Finkelstein (1983) that deposition occurs on straight coasts when a large amount of littoral drift becomes trapped up-drift of a boundary, usually an inlet or estuary mouth. In order to maintain the equilibrium, the down-drift limb of the inlet is subjected to erosion and migration of the inlet laterally. Such a scenario has been explained along the Mangalore coast of India (Avinash Kumar et al. 2010). If the accumulation of sediment at the up-drift arm completely balances the erosion at the down-drift end, a 'straight' inlet develops. It is observed that at present the proximal end of Kodi Bengre spit is stabilized in the north-south direction as this end is connected to the land, whereas the distal end of the Oddu Bengre spit is continuously subjected to the dynamical river mouth processes (Fig. 4).

Erosion / accretion pattern of estuarine banks

Based on estimation of width and areal extent of erosion/accretion pattern, we find that Right bank (Rb) of the estuary is subject to net erosion and the Left bank (Lb) to net accretion. Along Rb, erosional width ranges from 4 to 177 m whereas, accretion ranges from 3 to 42 m only (Fig. 4a). Block-wise area subject to erosion varies from 0.4 acre (block-4) to 37 acres (block-11). Erosion is relatively higher at blocks 11, 13 and 17 and lower at blocks 2, 4, 6, 7, 9, 12, 15 and 19. Remaining blocks (3, 5, 8, 10, 14, 16, 18 and 20) are subject to minor accretion (Fig. 4b). Along Lb, the width of accretion ranges from 5 to 136 m and erosion from 4 to 39 m (Fig. 4c). The area subject to accretion varies from 3 acres (block-1) to 22 acres (block-13). But, major accretion has been noticed at blocks 2, 13 and 15 and minor accretion at blocks 1, 4, 6, 8, 10 and 11. The remaining blocks (3, 5, 7, 9, 12 and 14) are subject to minor erosion only (Fig. 4d). Erosion and accretion pattern indicates that estuarine mouth has migrated, and adjacent spits are responsible for changes in bank morphology.

Origin of fluvial / estuarine islands

According to Stanford et al. (1996), fluvial system is a continuum of eight biophysical environments as shown in Fig. 6. In general, estuarine islands are found close to estuarine inlets, particularly in cases where the tidal energy is dominant over the fluvial and/or wave energy (Dalrymple and Zaitlin 1989; Dalrymple et al. 1992) and formed in tidal environments (Gomez and Perillo 1992; Fitzgerald et al. 2000; Bastos et al. 2002). Hence, estuarine islands are the result of stabilization and growth of shoals due to gradual accumulation of sediment brought by river and

eventually drifted into the estuary by waves and tidal currents. Some of the islands under study, namely, Gudderi Kambla, Padu, Mudu and Mavina might have been formed by detachment of a part of landmass from the mainland. There are a few shoals covered with vegetation towards southeast of the Parengi S, northwest of the Nayakra and east of the Mudu islands. Some of these shoals may grow larger, get stabilised and become inhabited in due course.

Morphological and evolutionary changes of islands

Six braided islands (I-VI) and three shoals are found close (~2-4 km) to the estuarine mouth and another group of nine braided islands (VII-XV) are found further southeast of the estuarine mouth (Fig. 1). Morphological and evolutionary changes in shape, orientation, areal extent of erosion/accretion, magnitude of migration and present elevation of a few islands with respect to the mean sea-level (MSL) are quantified and discussed in this section.

In 1967, areal extent of the *Parengi N (I) island* was about 6.34 acres and oriented in NNW-SSE direction (Figs. 7a and 8). This island became elongated, changed its orientation in the N-S direction and the area has been increased by 1.56 acres in 1997. From 1997 onwards, it remained almost stable (Table 1). Presently, it measures ~335 m in length, ~114 m in width and exposed to ~8 m from the MSL. The *Parengi S (II) island* is located south of the Parengi N island. The areal extent of this island was about 11.68 acres in 1967 and oriented in the N-S direction. Its area is increased by 2.32 acres, especially on its western and southern sides between 1967 and 1997 (Figs. 7a and 8). But during 1997-2005, this island was subject to erosion and its area reduced by 1.2 acres mainly along the southern and western sides (Table 1). The *Pinthru (III) island* is found parallel (with a gap of ~60 m) to the Oddu Bengre spit. In 1967, the spit was 288 m long and 60 m wide with an area of 4.94 acres. It was elongated and oriented in NNW-SSE direction (Figs. 7a). Whereas, this island has been shifted towards west by ~85 m and widened ~115 m, thereby it's area has increased by 1.96 acres during 1967-1997 (Table 1). From 1997 onwards, it was subject to minor erosion on its southeast and western sides (Fig. 7a). Presently, it is oriented in NW-SE direction and exposed to 8.5-9.5 m from the MSL.

The *Kiniyara (IV) island* is linear in shape and found in the middle of the estuary. In 1967, it measured ~310 m in length, 38-103 m in width and ~7 acres in area. After 30 years, it prograded by 80 m in northwest headward direction and ~45 m on the western side, thereby it increased in area by ~3.6 acres. Whereas, from 1997 onwards, minor erosion has been recorded along the periphery and its areal extent has been reduced by ~1 acre (Table 1). Topographically, this island is exposed by 4.5 m in northwest to 7 m in southeast from the MSL. In general, in the last 38 years period, the shape of

the Kiniyara island (IV) has changed from oval to rectangular, and shifted towards SW direction by ~38 m (Fig. 7a). The *Nayakra (V) island* is found towards north of the Kiniyara island and oriented in NW-SE direction. During 1967-1997, the areal extent of this island is upgraded by ~5 acres, while its width has been prograded by 17-64 m on eastern side and 13-61 m on western side. But, 1997 onwards, recession has been recorded all along its periphery. In 1967, the northwestern part of this island was rounded in shape, later during 1967-1997 it has been deformed to L-shape and grown towards NW direction (Fig. 7a). Presently, it extends in length by about 682 m and 40-185 m in width which is exposed by 5.7 m at NW part, 7 m at SE part and ~9 m in the middle part from the MSL. It is expected that the Parengi N island is acting as a barrier for the water currents, therefore the Nayakra island would continue to grow on its northwestern tip that eventually may join with the former one in future (Figs. 4 and 7a). The *Sahibra (VI) island* is located 70 m away from southeast of the Nayakra island. During 1967-1997, the island has shifted in the NE by 30-55 m and grown in the NW direction by ~40 m, thereby it's area has increased by 1.4 acres (Fig. 8). However, from 1997 onwards, erosion has been recorded along its NW and SE parts.

The *Gudderi Kambla (VII) island* was reduced by 0.8 acres and shifted ~70 m in southwest direction, during 1967-1997 (Table 1; Fig. 7b). From 1997 onwards, minor accretion has been recorded on eastern part of this island. Presently, it measures 500 m in length, 20-145 m in width and orientated in NW-SE. The Baligera (VIII) island is medium in size which is situated towards east of the Gudderi Kambla and oriented in EW direction. The island has shifted southwards by 60 m and prograded in EW direction, thereby area has been upgraded by 2.5 acres, during 1967-1997. However, from 1997 onwards, minor erosion has been recorded on all the parts of this island except northern part, where accretion has been noticed (Table 1; Fig. 7b). Presently, it measures ~712 m in length, 62-281 m in width and exposed by 9 m (on its east and west) to ~10 m (in the centre) from the MSL.

The *Padu (IX) island* is the second largest island in size. During 1967-1997, this island was subjected to severe erosion along the periphery especially on its west and lost a major landmass of ~24 acres (Table 1; Figs. 7b and 8). During the same period, about 1/10th part of the landmass (~10 acres) has been detached from the main island. From 1997 onwards, it is subjected to further erosion along the periphery and its areal extent has reduced by ~4 acres. At present, it measures ~100 acres with a length of 1150 m and width of 180-777 m which exposed by 9 m (in north) to 11.8 m (in south) from the MSL. The *Timmana (X) island* located towards northeast of the Padu island is medium in size and oriented in NW-SE direction. During 1967-1997, this island has prograded by 20-100 m all along its periphery except in the northwest part, where 10-40 m recession has been

recorded. However, during 1997-2005, minor erosion has been noticed at a few places (Table 1; Fig. 7b). In general, the eastern portion of this island is accreting and widening. Presently, it measures 740 m in length and 286 m in width while surface elevation from MSL varies from 8.2 m to 11.8 m in northwest and central part of this island, respectively. The *Shinesi (XI) island* is oriented in WNW-ESE direction and almost parallel to the Timmons island with a gap of 30 m. During 1967-1997, it has migrated towards east and its area has been reduced by ~0.4 acres (Table 1). From 1997 onwards, minor erosion and accretion trends were noticed all along its periphery. During the past 38 years, orientation of this island has been changed by $\sim 6^\circ$ (Fig. 7b). Presently, the island measures a length of 625 m and width of 110 m which is exposed by 10-11 m from the MSL.

The *Mudu (XII)* is the largest among all the fifteen islands which is located southeast of the Timmana and Shinesi islands (Figs. 1 and 7b). The areal extent of this island was ~151 acres in 1967. In the past 30 years, the island has increased by 11 acres and subsequently decreased by 3 acres during 1997-2005 (Table 1). Presently, it measures a length of ~1500 m and width of 110 to 615 m, and oriented in NW-SE direction (Fig. 7b). The *Chittara (XIII) island* is one of the small islands located towards north of the Mudu island. The areal extent of this island has increased from 4.9 acres to 8.1 acres during 1967-1997 while minor reduction has been recorded during 1997-2005 (Table 1; Fig. 8). During the past 38 years, shape of the island has been changed from oval to elongated and oriented in NW-SE direction (Fig. 7b). The *Bari (XIV) island* is also one of the small islands which has undergone minor changes in its areal extent and migrated towards north by ~70 m (Table 1; Fig. 7b). The *Mavina (XV) island* is the medium sized, oriented in NW-SE direction and found on the extreme eastern side of the estuary (Fig. 1). The area of this island has been increased by 5.5 acres, during 1967-1997, but slightly decreased during 1997-2005 (Table 1; Figs. 7b and 8). Finally, the island is prograding in its northern side towards the mainland and suspected that it may join with the mainland in due course of time (Fig. 1).

Impact of floods on estuarine islands

All the braided islands (I-XV) and shoals of the Swarna estuary are partially or fully flooded during the highest high tide, heavy rains in southwest monsoon and/or sea-level rise. Higher tidal fluctuation and flood deposited large amount of sediment derived from tributaries and bank erosion, filling the former channel and creating a fresh layer of coarse sand, fine gravel on many of the pre-flooded bottom land. From the IDW interpolation model, it is found that the gradient of the estuarine basin is towards north (i.e. from Lb to Rb). Therefore, right bank is subject to erosion and left bank

to accretion. As a result, the land along Lb is prograding, and water channel is shifting towards Rb (Fig. 4).

It has been estimated that more than 80% of Parengi N, 36% of Parengi S, 22% of Pinthru, 50% of Kinyara, 10% of Nayakra and 10% of Sahibra islands (I-VI) will be flooded if water level rises by 0.7 to 1.0 m (Fig. 9a) and 70 to 80% area of all the shoals will be submerged if water level rises by the same magnitude. From 1967 onwards all these islands (except Sahibra) were subject to continuous erosion along their right sides which are comparatively elevated than the left sides. However, most of the low-lying flooded areas of islands are prograded and shifted further towards Lb (Fig. 7a).

Another group of eight braided islands (VII-XIV) are comparatively larger, stable and vary from 7 to 15 m in height with respect to MSL. The islands close to the Lb (VII-X and XII) are relatively at higher elevation compared to that found in the middle of the estuary (XI) and those close to the Rb (XIII and XIV). Those close to the Lb are dipping towards north, while, the remaining ones are dipping towards both north and south (Fig. 9b). Hence, the possibility of flooding would be more on the northern portion of the islands close to the Lb. In this case, it has been estimated that 30-40% of Gudderi Kambla, 24-48% of Baligera, 4-5% of Padu, 1.5-7% of Timmana, 10-40% of Shinesi, 1-4% of Madu, 13-60% of Chittara and 15-68% of Bari islands would be flooded if the water level increases by 0.7 to 1.0 m, whereas, the Mavina (XV) island and a shoal found southeast of the Madu island (Fig. 10) with an elevation ranging from 4 to 13 m would be flooded relatively less (2-10% of the Mavina island and 10-20% of shoal) if water level raises by 0.7 to 1.0 m. Hence, since 1967 all the nine islands (VII-XV) shifted towards Rb and accretion occurred along their right side, where flooded low-lying area is found to be dominant.

Conclusions

Coastal and tidal currents off Swarna estuary contribute sediments to the adjacent barrier spits, and make the spits to grow in the direction of longshore sediment transport. This, in turn, must be responsible for erosion and accretion of Rb and Lb, respectively and change in morphology and orientation of islands. Currents and southerly littoral drift along the Kodi Bengre spit act as barriers for the drift. Hence, the estuarine mouth has migrated towards southeast due to erosion at the distal end of the Oddu Bengre spit and accretion at the Kodi Bengre spit. Areal extent of most of the islands increased during 1967-97 period, but from 1997 onwards they are subject to net erosion. In

general, the islands close to the estuarine mouth (I-VI) are affected by erosion especially along their right side, and the remaining islands are subject to accretion along their right side.

The possibility of flooding will be higher for those islands which are located close to Rb than those close to Lb. On an average, 20-30% of the area of all braided islands would be flooded, if water level rises by 0.7 to 1.0 m. North and eastern sides of the Parengi N, Parengi S and Pinthru islands, and north and western sides of the Kinyara and Nayakra islands would get affected as these islands are less elevated. On the contrary, islands close to the Lb (Gudderi Kambla, Baligera, Padu, Timmana and Mudu) would get affected by floods very marginally as they are having relatively higher elevation. The study area is densely populated and the inhabitants of the islands/barrier spits are facing problems like flooding during high tide and southwest monsoon, sea water intrusion and bank erosion.

Acknowledgements

The first author (AK) thanks the Council of Scientific and Industrial Research (CSIR), India, for awarding Senior Research Fellowship. The authors are grateful to the Department of Science and Technology, Government of India, for funding a research grant (No. ES/11/720/2003). They wish to thank Mr. Sudhakar, for providing the boat and Mrs. Rajesh and Suresh for extending their help during the field surveys. They thank Ms. Deepika B. and Mr. A. K. Warriar, Department of Marine Geology, Mangalore University for extending assistance during the preparation of this manuscript.

Authors acknowledge anonymous reviewers and Dr. Gunter Doerhoefer, Editor-in-Chief, for their insightful comments and suggestions on the previous draft, which improved the quality of the paper.

References

Achyuthan H, Baker VR (2002) Coastal response to changes in sea-level since the last 4500 BP on the east coast of Tamilnadu, India. *Radiocarbon* 44:137-144.

Aguilar FJ, Aguilar MA, Aguera F (2007) Accuracy assessment of digital elevation models using a nonparametric approach. *Int J Geogr Inf Sci* 6:667-686.

Allen GP, Posamentier HW (1993) Sequence stratigraphy and facies model of an incised valley fill: the Gironde Estuary, France. *J Sed Pet* 63:378-391.

Avinash Kumar, Narayana AC, Jayappa KS (2010) Shoreline changes and morphology of spits along southern Karnataka, west coast of India: A remote sensing and statistics-based approach. *Geomorphology* 120:133-152.

Bastos AC, Kenyon NH, Collins MB (2002) Sedimentary processes, bedforms and facies associated with a coastal headland: Portland Bill, southern UK. *Mar Geol* 187:235-258.

Bonham-Carter G (1994) Geographic information systems for geoscientists: modelling with GIS. 1st Edition Computer methods in the geosciences, Oxford, New York. Pergamon 13, 398p.

Burrough PA, McDonnell R (1998) Principles of geographical information systems. Spatial information systems, New York, Oxford University Press, xiii, 333p.

Chakrabarty P (1991) Process response system analysis in the macro and meso-tidal coastal plains of Eastern India. *Mem Geol Soc India* 22:165-181.

Chandramohan P, Jena BK, Sanil Kumar V (2001) Littoral drift sources and sinks along the Indian coast. *Curr Sci* 81:292-297.

Chen LC, Rau JY (1998) Detection of shoreline changes for tideland areas using multi-temporal satellite images. *Int J Remote Sens* 19:3383-3397.

Cook AE, Pinder JE (1996) Relative accuracy of rectification using co-ordinates determined from maps and Global Positioning System. *Photogramm Eng Rem S* 62:73-77.

Dalrymple RW, Zaitlin BA (1989) Tidal sedimentation in the macrotidal Cobequid Bay-Salmon River Estuary, Bay of Fundy. *Field Guide*, 2nd Int. Res. Symposium Clastic Tidal Deposition, Calgary, Alberta, Canadian Society of Petroleum Geologists, 84p.

Dalrymple RW, Zaitlin BA (1994) High-resolution sequence stratigraphy of a complex, incised valley succession, Cobequid Bay – Salmon River estuary, Bay of Fundy, Canada. *Sedimentology* 41:1069-1091.

Dalrymple RW, Zaitlin BA, Boyd RJ (1992) Estuarine facies models: conceptual basis and stratigraphic implications. *J Sed Pet* 62:1130-1146.

Finkelstein K (1983) Cape formation as a cause of erosion on adjacent shoreline. *Proc. Symp. Coastal and Ocean Management*. American Society of Civil Engineers, New York, 620-640.

Fitzgerald DM, Buynevich IV, Fenster MS, Mckinlay PA (2000) Sand dynamics at the mouth of a rock-bound, tide-dominated estuary. *Sediment Geol* 131:25-49.

Gomez EA, Perillo GME (1992) Lorgo Bank: a shoreface-connected linear shoal at the Bahia Blanca Estuary entrance, Argentina. *Mar Geol* 104:193-204.

Jayappa KS, Vijaya Kumar GT, Subrahmanya KR (2003) Influence of coastal structures on the beaches of southern Kannada, India. *J Coastal Res* 19:389-408.

Jouanneau JM, Latouche C (1981) *The Gironde Estuary*. E. Schw. Verlagchh., Stuttgart, 115p.

Knebel HJ, Fletcher CH, Kraft JC (1988) Late Wisconsinan – Holocene paleogeography of Delaware Bay: a large coastal plain estuary. *Mar Geol* 83:115-133.

Lambin EF, Strahler AH (1994) Change-vector analysis in multitemporal space: a tool to detect and categorize land cover change processes using high temporal resolution satellite data. *Remote Sens Environ* 48:231–244.

Laurini R, Thompson D (1992) *Fundamentals of Spatial Information Systems*. London Academic Press.

Lillesand TM, Kiefer RW (2000) *Remote Sensing and Image Interpretation*. 4th Edition, New York: John Wiley & Sons, Inc.

Menon HB, Lotliker A, Nayak SR (2006) Analysis of estuarine colour components during non-monsoon period through Ocean Colour Monitor. *Estuar Coast Shelf S* 66:523– 531.

Quarmby NA, Cushnie JL (1989) Monitoring urban land cover changes at the urban fringe from SPOT HRV imagery in south-east England. *Int J Remote Sens* 10:951–963.

Sastri JS, Vethamony P, Swamy GN (1991) Morphological changes at Godavari delta region due to waves, currents and the associated physical processes. *Mem Geol Soc India* 22:139-151.

Sanil Kumar V, Pathak KC, Pednekar P, Raju NSN, Gowthaman R (2006) Coastal processes along the Indian coastline. *Curr Sci* 91:530-536.

Singh A (1989) Digital change detection techniques using remotely sensed data. *Int J Remote Sens* 10:989–1003.

Stanford JA, Ward JV, Liss WJ, Frissel CA, Williams RN, Lichatowich JA, Coutant CC (1996) A general protocol for restoration of regulated rivers. *Reg Riv Res and Manage* 12:391:413.

Titus J, Richman C (2000) Maps of lands vulnerable to sea-level rise: modeled elevations along the US Atlantic and Gulf Coasts. *Climate Res* 18:205–228.

Weismiller RA, Kristof SJ, Scholz DK, Anuta PE, Momen SA (1977) Change detection in coastal zone environments. *Photogramm Eng Rem S* 43:1533–1539.

Write LD, Coleman JM (1973) Variations in morphology of major river deltas as function of ocean waves and river discharge regimes. *American Association of Petroleum Geologists Bulletin* 5:370–398.

Yang, Xiaojun (2005) Remote sensing and GIS applications for estuarine ecosystem analysis: an overview. *Int J Remote Sens* 26:5347–5356.

Table 1. Changes in areal extent of the islands during the periods of 1967, 1997 and 2005

Name of islands	Area in acres			Net
	1967	1997	2005	changes
	1967	1997	2005	1967-2005
I - Parengi N	6.34	7.9	7.5	+1.16
II - Parengi S	11.68	14.0	12.8	+1.12
III - Pinthru	4.94	6.9	6.3	+1.36
IV - Kinyara	7.03	10.7	9.8	+2.77
V - Nayakra	14.83	20.0	18.5	+3.67
VI - Sahibra	4.80	6.2	5.1	+0.3
VII - Gudderi Kambla	13.09	12.2	12.6	-0.49
VIII - Baligera	27.53	30.1	28.7	+1.17
IX - Padu	128.79	104.6	100.4	-28.39
X - Timmana	28.99	31.4	30.8	+1.81
XI - Shinesi	13.05	12.6	12.3	-0.75
XII - Mudu	151.37	161.9	157.8	+6.43
XIII - Chittara	4.95	8.1	7.4	+2.45
XIV - Bari	8.28	8.5	7.4	-0.88
XV - Mavina	48.21	53.7	51.3	+3.09

Positive (+) and negative (-) sign indicate accretion and erosion, respectively.

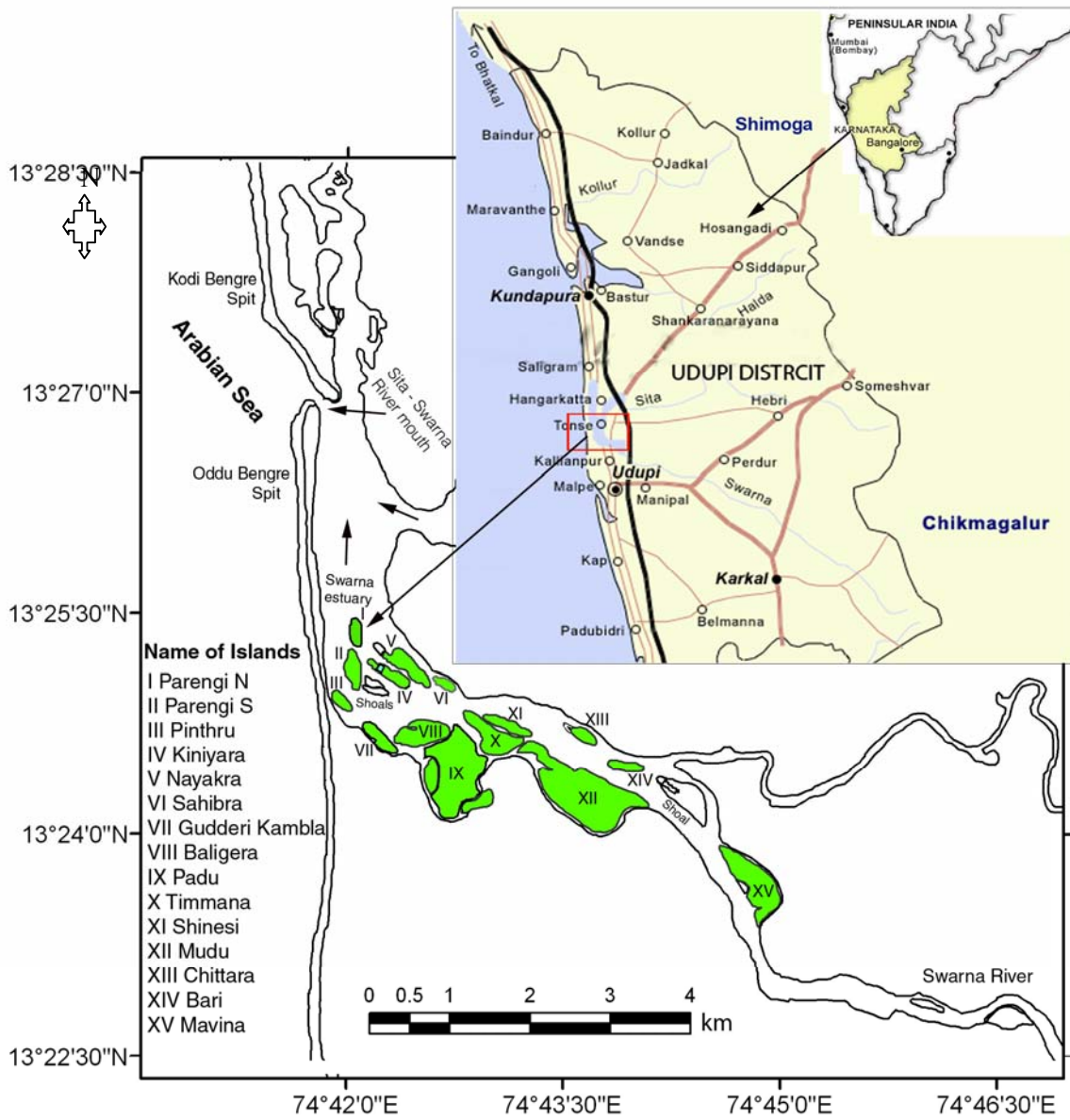
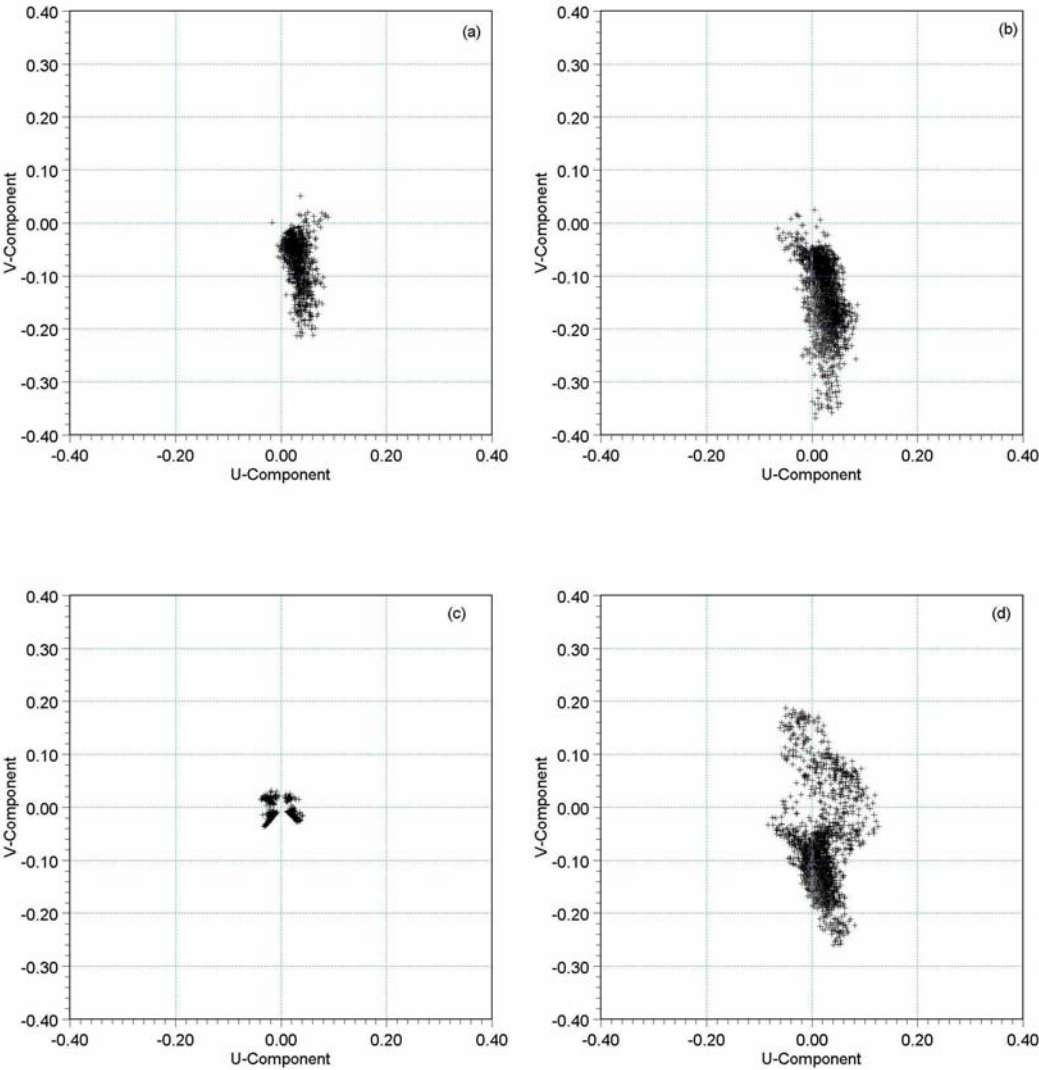


Fig. 1. Location map showing present morphological condition of the islands, spits and channels of the Swarna estuary

Fig. 2. Scatter plot of currents at 13°28'N and 74°38'E between 12 and 27 May 1997 (water depth = 12 m): (a) Surface currents, (b) Bottom currents. (c) Bottom currents between 9 and 24 Jan 1998 (water depth of 12 m), and (d) Current components between 12 April and 11 May 2007 (water depth of 13 m).



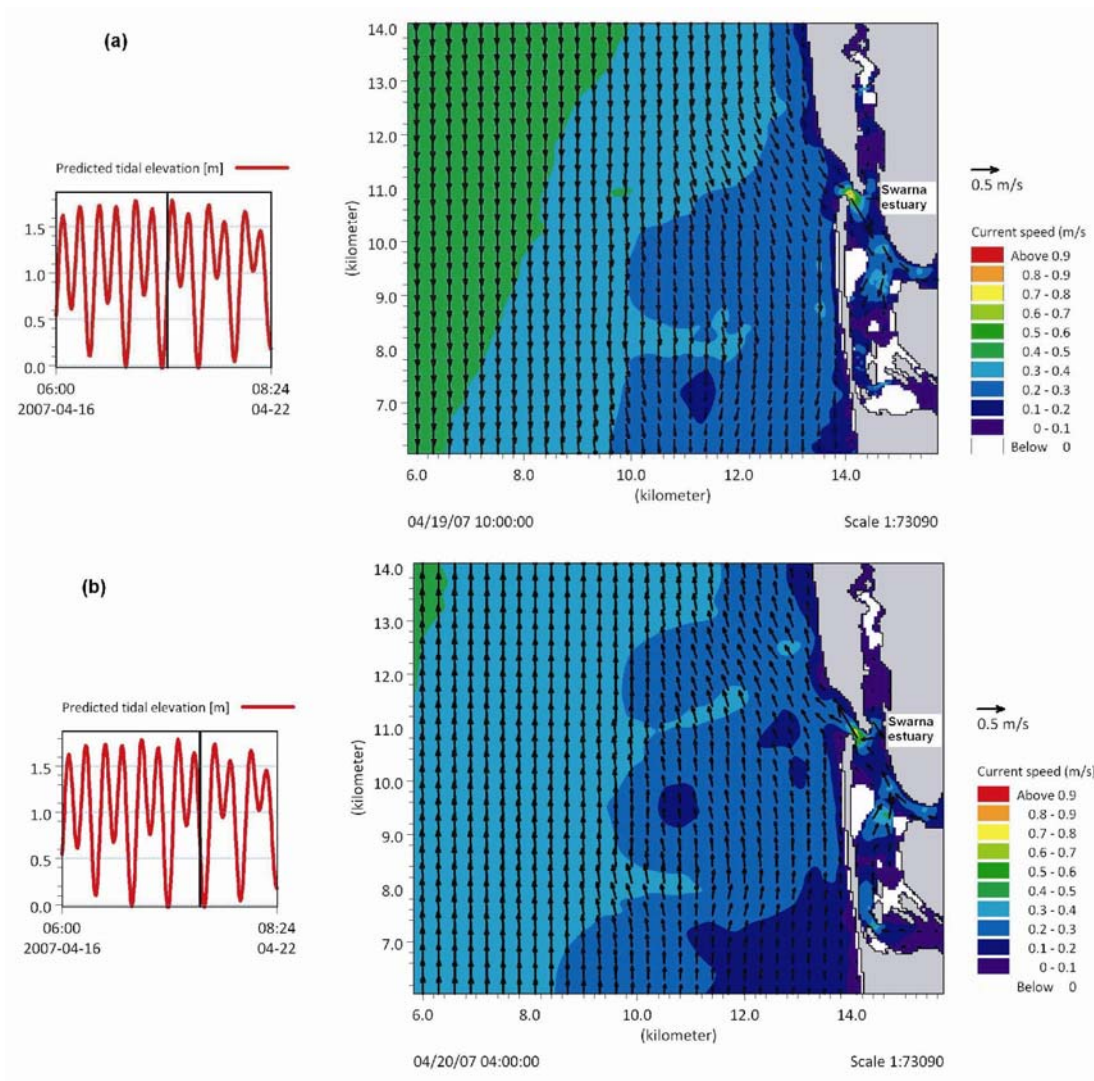


Fig. 3. A typical flow pattern around the Swarna estuary: (a) flood currents and (b) ebb currents. Corresponding tide elevations are also shown in these figures.

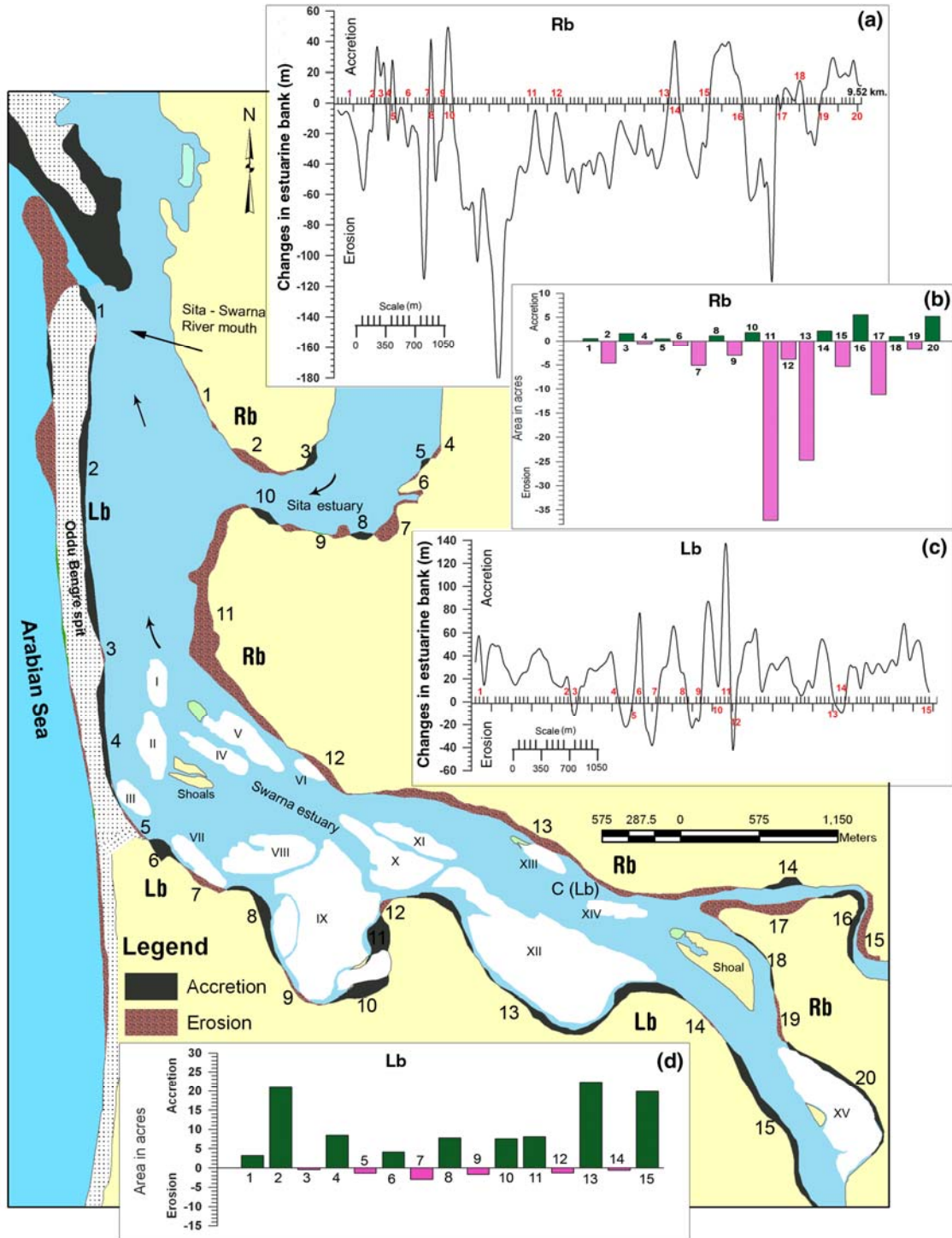


Fig. 4. Accretion/erosion patterns along the banks of the Swarna estuary during the past 38 years (1967-2005). The Right bank (Rb) is subjected to net erosion and the Left bank (Lb) is subjected to accretion. To estimate the width and areal extent of accretion/erosion patterns, the Rb and Lb have been divided into 20 and 15 blocks respectively. Width and areal extents of accretion/erosion are shown in profiles (inserts a and c) and bar diagrams (b and d) for the Rb and the Lb, respectively.

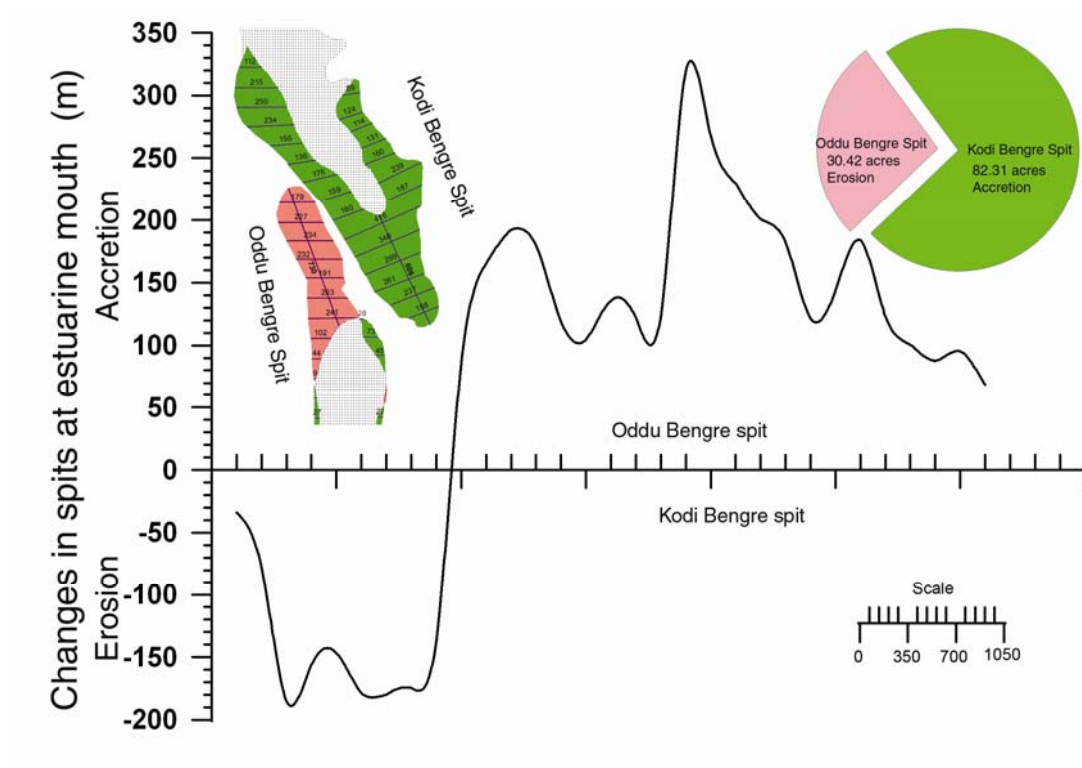


Fig. 5. Accretion/erosion patterns of spits and migration of estuarine mouth of the Sita-Swarna during the past 38 years (1967-2005). The estimated net accretion (~82 acres) and erosion (~30 acres) at the distal end of the Kodi and Oddu Bengre spits respectively are shown in the **vector and** Pie-diagram.

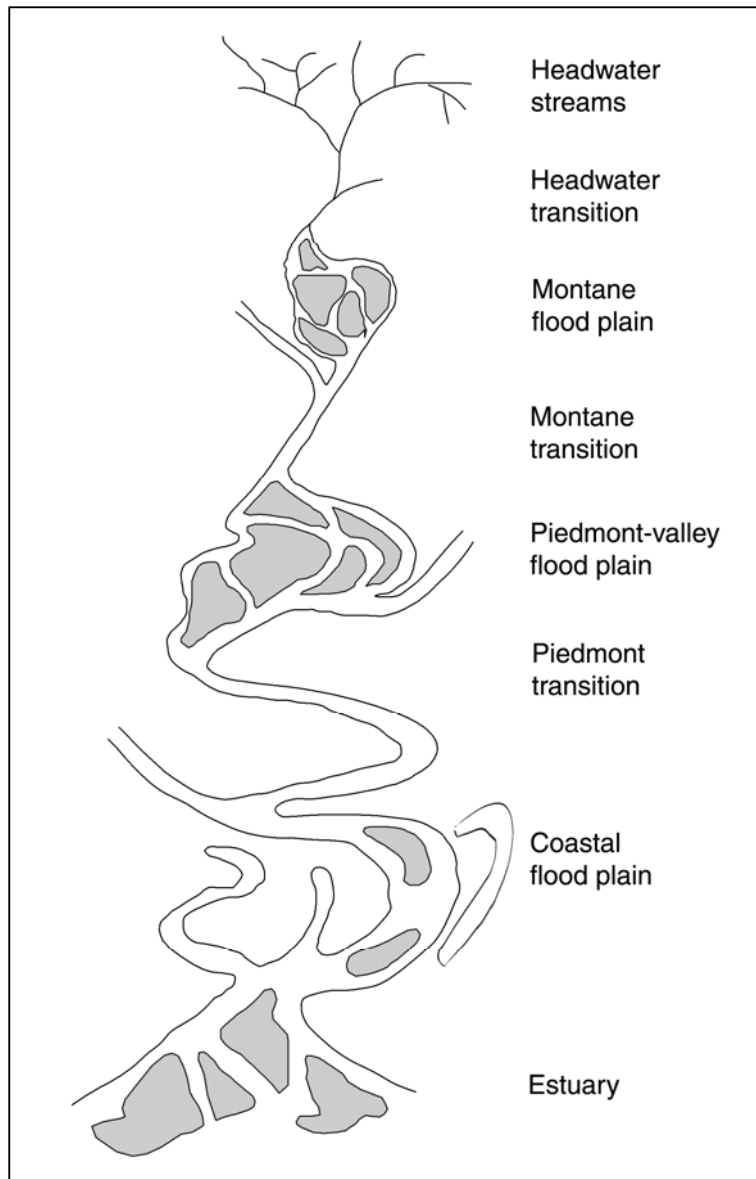


Fig. 6. Schematic drawing of the biophysical continuum for a river system, progressing from headwater streams of an alpine area, through the montane, piedmont-valley and coastal flood plains to an estuary (modified from Stanford et al. 1996).

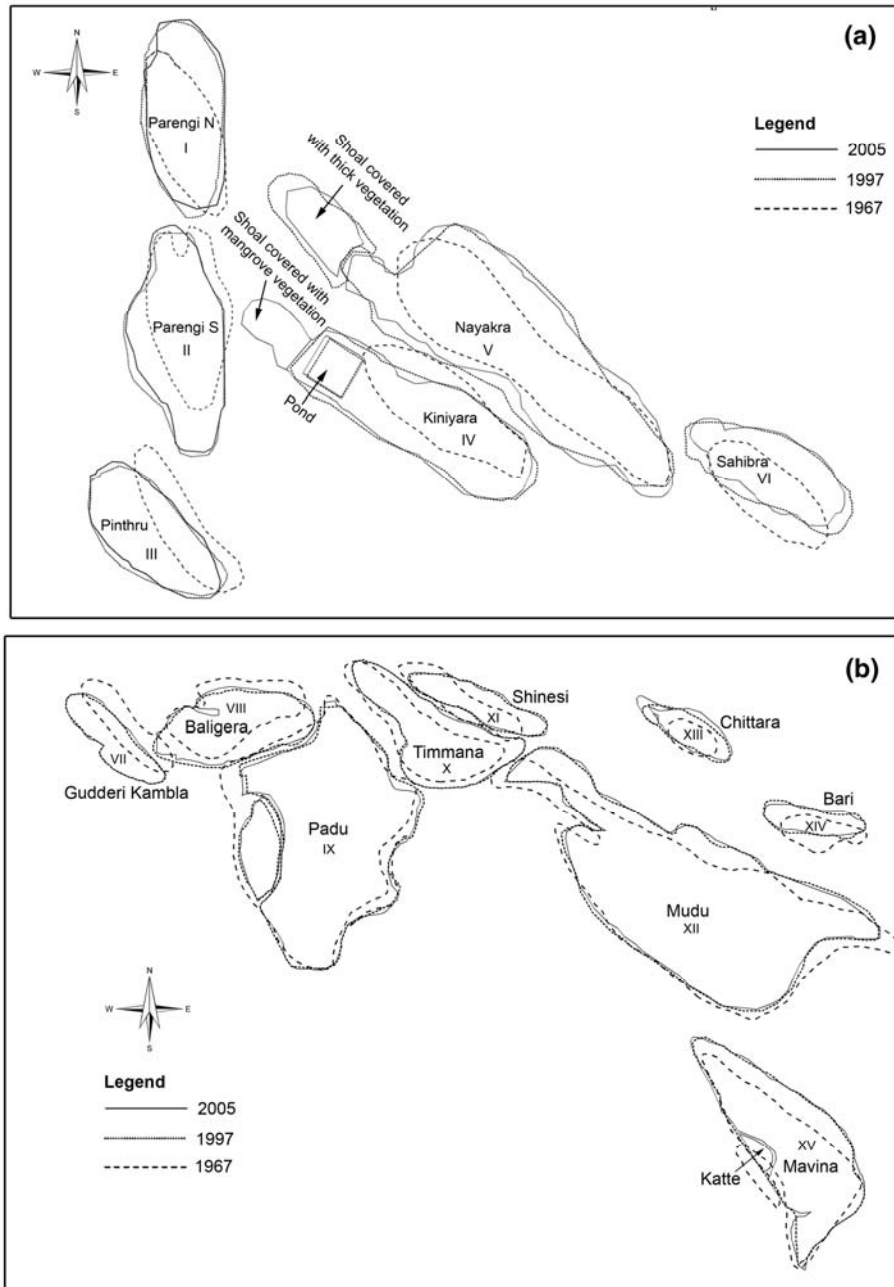


Fig. 7. In the past 38 years, changes in orientation and morphology of six medium to small islands (I-IV), located close to the Swarna estuarine mouth (a), and (b) changes in orientation and morphology of four small (VII, XI, XIII and XIV), three medium (VIII, X and XV) and two large (IX and XII) islands in the middle part of the Swarna estuary.

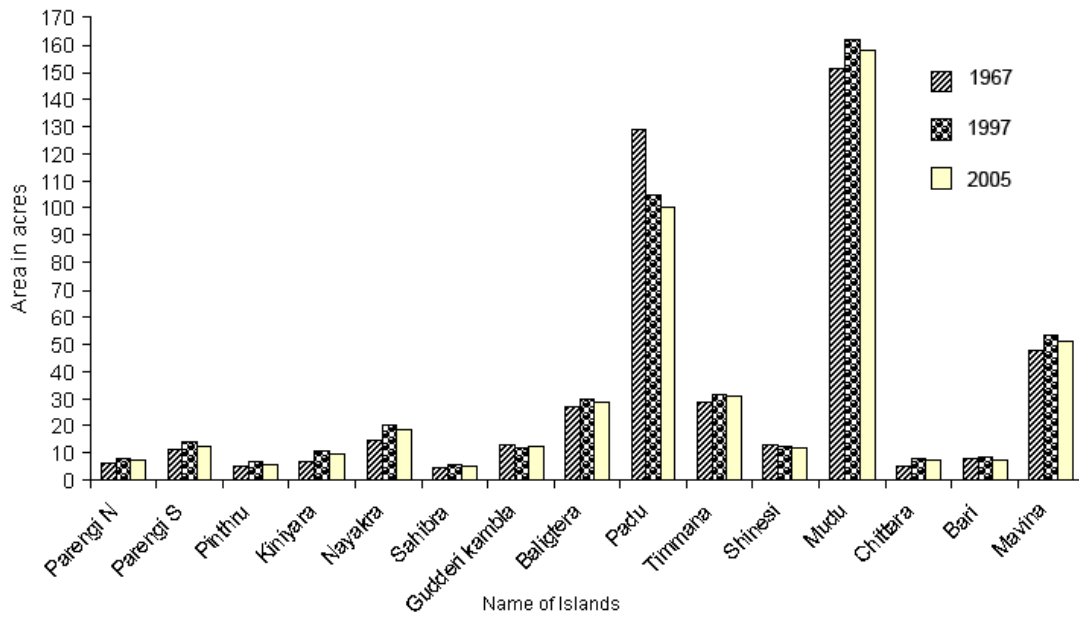
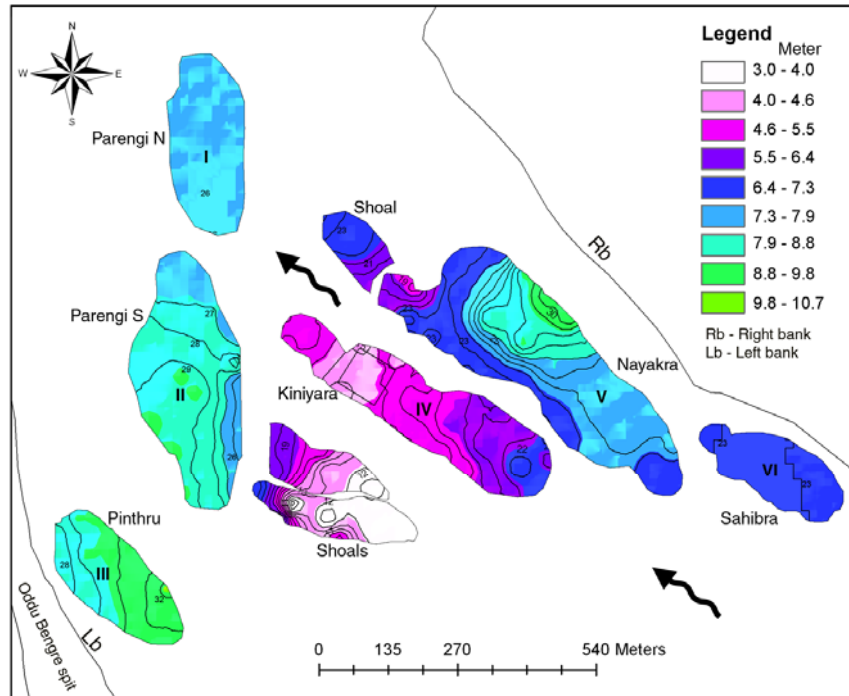
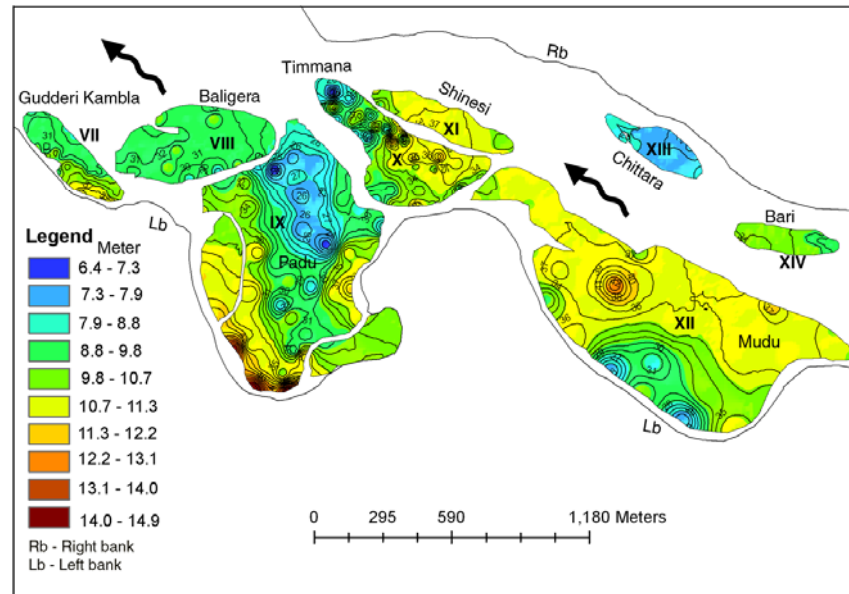


Fig. 8. Changes in areal extent of the islands show accretion trends at most of the islands except Gudderi Kambla, Padu and Shinesi islands where erosion has been recorded, during 1967-1997. Whereas, during 1997-2005, all the islands show decrease in their areal extent except Gudderi Kambla which shows minor increase in areal extent.



(a)



(b)

Fig. 9. Surface interpolation model, showing high resolution contours (at one foot interval) of various braided islands of the Swarna estuary. (a) Islands (I-VI) and shoals close to estuarine mouth where elevation ranges from 3.0 to 10.6 m (10 to 35 feet) from the MSL, and (b) Islands (VII-XIV) at middle part of the estuary, showing elevation ranges form 6.4 to 14.9 m (21 to 49 feet) from the MSL.

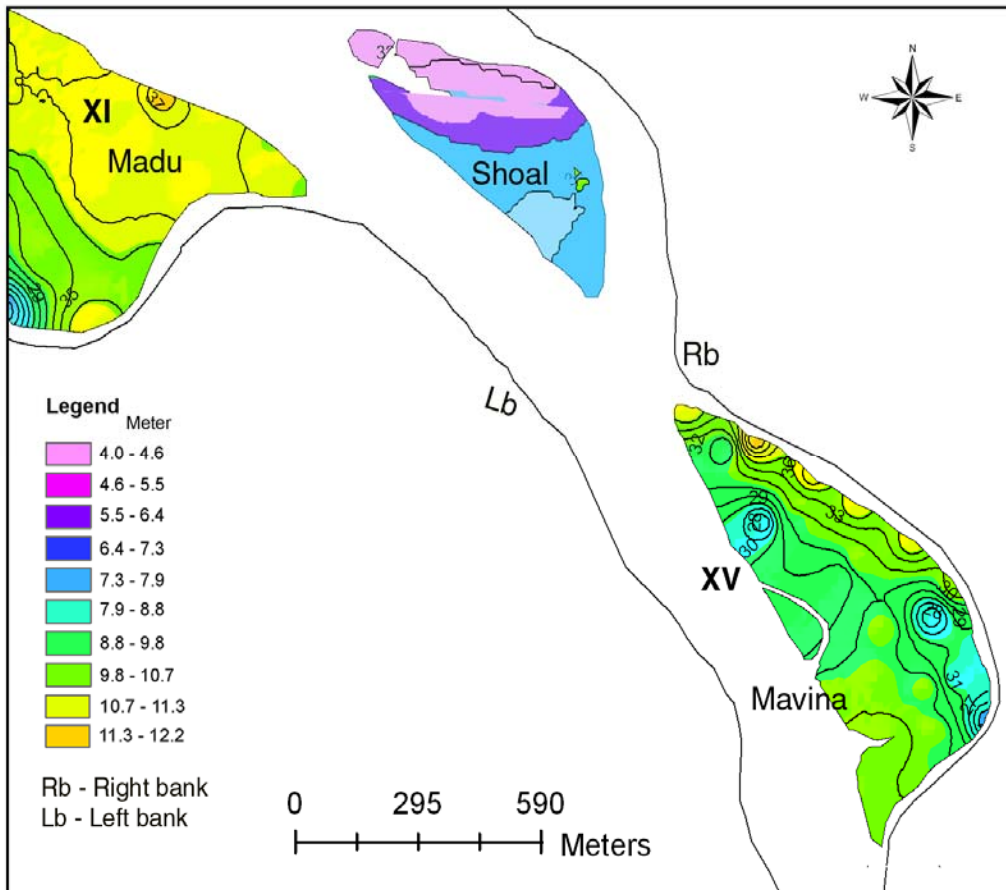


Fig. 10. Surface interpolation model, showing high resolution contours (at one foot interval) of the Mavina (XV) island and a shoal where elevation ranges from 3.9 to 11.2 m (13 to 37 feet) from the MSL.